The Novel Synthesis of $La_{0.8}Sr_{0.2}MnO_3$ Using the Michael-Addition Directed Hydrogelation of Acrylates for Materials Synthesis (MADHAMS) Method

Edwin H. Walker, Jr.,*,† Allen W. Apblett,‡ Ron Walker,† and Adam Zachary†

Department of Chemistry, Southern University and A & M College, P.O. Box 12566, Baton Rouge, Louisiana 70813, and Department of Chemistry, Oklahoma State University, Stillwater, Oklahoma 74078

Received July 2, 2004. Revised Manuscript Received September 15, 2004

This report describes the low-temperature synthesis of nanocrystalline perovskite oxide, $La_{0.8}Sr_{0.2}MnO_3$ (LSM), using the ammonium acrylate salt precursor gel method that employs 3,3′,3″-nitrilotripropionic acid (NTP) as the gelling agent. Due to its high degree of hydrogen bonding with water, NTP can absorb many times its own weight of water to yield a viscous liquid. Subsequent pyrolysis converts the mixture to the desired metal oxides. This preparative method has several advantages such as homogeneity, excellent control of stoichiometry, ease of handling, lower heating times and temperatures, and the production of uniform particle size and distribution. The synthesis of the LSM is achieved in as little as 10 hours (400 °C) with uniform distribution of particles that are 25 nm in size.

Introduction

Perovskite ionic conductors have interesting and useful chemical properties in addition to their ability to transport ions, and these characteristics have led to applications in oxygen permeable membranes[1−3] and gas sensors, and as electrocatalysts.[4,5] The most widely used cathode material for solid oxide fuel cells (SOFC) based on zirconia electrolytes is Sr-doped $LaMnO_3$ (LSM). LSM exhibits a high electronic conductivity and shows much less tendency to react with the commonly used zirconia-based electrolytes than other perovskite materials. However, LSM has a low ionic conductivity in air compared to zirconia- or ceria-based electrolytes.[6] LSM becomes reduced and develops ionic conductivity only at high overpotential.[7] Recently, LSM has received great attention as a cathode and interconnection material for solid oxide fuel cells.[8] Sr-substituted $LaMnO_3$, $LaFeO_3$, and $LaCoO_3$ show high oxidation activity, and $La_{0.6}Sr_{0.4}MnO_3$ is almost as active as Pt/Al_2O_3. Efforts are being made to improve the catalysis by synthesizing nanocrystalline $La_{1-x}Sr_xMnO_3$, which results in particles with very large specific surface area and corresponding greater catalytic activity.

With the expanding interest in the oxidation of hydrocarbons using perovskite-type oxides as catalysts and in the development of nanocrystalline metal oxides that possess unique electrical, magnetic, structural, and catalytic properties, a great deal of research has been focused on the development of novel methods of preparation[9−14] for these metal oxides. Interestingly, the properties of these nanocrystalline metal oxides have been found to be influenced by their method of preparation. The production of perovskites with highly desirable properties such as fast ion oxide conduction, colossal magnetoresistance, and catalytic activity requires nanocrystalline particles of uniform morphology and particle size distribution.[15,16] It is well established that the morphology and particle size distribution are important factors that determine the physicochemical properties of the perovskite materials, yet the lack of a suitable, consistent method of preparation that can be readily scaled-up has hampered research in this field. Perovskite oxides have been synthesized by a variety of methods including the use of both inorganic[17−21] and metallo-organic precursors [22−26] that thermally decom-

* To whom correspondence should be addressed. E-mail: edwin_walker@cxs.subr.edu. Phone: 225-771-3717. Fax: 225-771-3992.
† Southern University and A & M College.
‡ Oklahoma State University.

(1) Tseng, A. C. C.; Bevan, H. L. *J. Electroanal. Chem.* **1973**, *45*, 429.
(2) Manoharan, R.; Shukla, A. K. *Electrochim. Acta* **1985**, *30*, 205.
(3) Meadowcroft, D. B. *Nature* **1970**, *226*, 847.
(4) Teraoka, Y.; Zhang, H. M.; Furukawa, S.; Yamazoe, N. *Chem. Lett*. **1985**, 1743.
(5) Teraoke, Y.; Nobunaga, T.; Yamazoe, N. *Chem. Lett*. **1988**, 503.
(6) Steele, B. C. H.; Carter, S.; Selcuk, A.; Chater, R.; Kajda, J.; Kilner, J. A. *Solid State Ionics* **1992**, *53*, 597.
(7) Gharbage, B.; Pagnier, T.; Hammou, A. *J. Electrochem. Soc.* **1994**, *141*, 2118.
(8) Srinvasan, S.; Dave, B. B.; Murugeamoorthi, K. A.; Parthasarthy, A. Appleby, A. J. In *Fuel Cell Systems*; Blomen, L. J. M. J., Mugerwa, M. N., Eds.; Plenum: New York, 1993.
(9) Das, R. N.; Pathak, A.; Pramanik, P. *J. Am. Ceram. Soc.* **1998**, *81*, 3357.
(10) Adak, A.; Pathak, A.; Pramanik, P. *J. Mater. Sci. Lett.* **1998**, *17*, 559.
(11) Pati, R. K.; Pramanik, P. *J. Am. Ceram. Soc.* **2000**, *83*, 1822 .
(12) Pramanik, P. *Bull. Mater. Sci.* **1996**, *18*, 819.
(13) Pramanik, P. *Bull. Mater. Sci.* **1996**, *19*, 957.
(14) Suresh, K.; Patil, K. C. *J. Solid State Chem.* **1992**, *99*, 12.
(15) Miyamoto, N.; Tanabe, I. *Denki Kagaku* **1990**, *58*, 663.
(16) Reimers, J. N.; Dahn, J. R. *J. Electrochem. Soc.* **1992**, *139*, 2091.
(17) Vidyassagar, K: Gopalakrishnan, J.; Roa, C. N. *Inorg. Chem.* **1984**, *23*, 1206−1210.
(18) Anegelov, S.; Zhecheva, E.; Petrov, K.; Menandjiev, D. *Mater. Res. Bull.* **1982**, *17*, 235.
(19) Petrov, K.; Markov, L.; Ioncheva, R. *J. Mater. Sci. Lett.* **1985**, *4*, 711.
(20) Klissurski, D.; Uzunova, E. *Chem. Mater.* **1991**, *3*, 1060.
(21) Wright, P. A.; Natarajan, S.; Thomas, J. M.; Gai-Boyes, P. L. *Chem. Mater.* **1992**, *4*, 1053.

10.1021/cm0489385 CCC: $27.50
Published on Web 11/18/2004

pose at low temperatures; the coprecipitation of ions in solution;[27−34] the ceramic method in which metal oxides, metal carbonates, and metal hydroxides are ground and heated to very high temperatures for long periods of time;[35−37] and sol−gel processes.[38,39] These methods often suffer from several disadvantages such as inhomogeneity, irregular morphology, large particle size with a broad particle distribution, and poor control of stoichiometry, while other methods involve the use of expensive, air-sensitive reagents, organic solvents, or require multistep processes. Also, there are still other additional routes, such as hydrothermal techniques, plasma spray decomposition, combustion of metal nitrates and urea, freeze-drying of sulfate solutions, controlled hydrolysis of metal alkoxides, decomposition of organometallic compounds in supercritical fluids, multi-metallic alkoxide precursors, and aerosol methods that are available for the preparation of nanocrystalline perovskite powders. However, the materials scientists involved in the development of new synthetic routes are still faced with a major challenge of finding procedures that are both affordable and versatile.[11]

This report describes the low-temperature synthesis of the nanocrystalline perovskite oxide, $La_{0.8}Sr_{0.2}MnO_3$ (LSM), using the ammonium acrylate salt precursor gel method recently developed by the Walker group[40] that employs 3,3′,3″-nitrilotripropionic acid (NTP) as the gelling agent. Due to its high degree of hydrogen bonding with water, NTP can absorb many times its own weight of water to yield a viscous liquid. It is generated in a mixture of metal acrylates by the Michael addition of ammonia with the vinyl group of acrylic acid. This generates a hydrogel in which the metal ions are distributed homogeneously throughout the hydrogen-bonded network of NTP. Subsequent pyrolysis converts the mixture to the desired metal oxides. This preparative method has several advantages over the previously mentioned methods such as homogeneity, excellent control of stoichiometry, ease of handling, lower heating times and temperatures, and the production of uniform particle size and distribution. It is also very inexpensive, since it utilizes low-cost starting materials. Synthesis of the LSM is achieved in as little as 10 hours (400 °C) with uniform distribution of particles that are 25 nm in size.

Experimental and Instrumental

Acrylic acid, lanthanum acetate, manganese acetate, and strontium hydroxide were purchased from Aldrich Chemicals. Ammonium hydroxide (29% NH_3) was purchased from VWR Scientific Products. The flash-evaporator (Buchler Instruments) was chilled with a Sargent-Welch water bath pumped with a Welch-Duo-Seal vacuum pump for evaporations. Compounds were dried using a NAPCO vacuum oven (model 5831) equipped with a Sargent-Welch director vacuum pump. Deionized water was prepared using the Solution 2000 water purification pure system and the Simple Solution 2000 compact reverse osmosis Type 1 DI water purification system. Pyrolysis of perovskite precursor was performed using the Fischer Scientific Iso-temp muffle furnace with a temperature range from 400 to 1100 °C. Infrared analysis was performed utilizing the Nexus 870 FTIR using the Spectra-Tech Thunderdome germanium single-crystal ATR and Omnic software. The single-crystal X-ray analysis was performed on a Nonius Kappa CCD diffractometer with a cryogenic apparatus for performing low-temperature structure determinations. XRD measurements were acquired utilizing the Siemens D5000 Kristallotex, housed at the Geology and Geophysics XRD Laboratory of Louisiana State University (Baton Rouge, LA) or a Bruker D8 Advance diffractometer at Oklahoma State University. Crystalline phases were identified using the PDF-2 database of the International Centre for Diffraction Data. The X-ray reflections were profiled with a Peason 7 model using Topas P Version 1.01 software. The profiles of the standard (highly crystalline hematite) and the sample were input into the Win-Crysize Version 3.05 program that used the single peak evaluation method to determine crystallite size. The TEM analysis was performed on a JEOL JEM 2010 transmission electron microscope operating at 200 keV. The ^1H and ^{13}C NMR measurements were acquired in 600 μL of D_2O at 25 °C on a Bruker DRX 500 MHz spectrometer equipped with an inverse XYZ gradient and a 5-mm Bruker probe. The ^{13}C signal assignments were based on the initial delineation of the individual proton spin systems within each molecule using a variety of 2D techniques. These techniques include the following: gradient versions of the correlation spectroscopy double-quantum filtered method [COSY (DQF−COSY)],[41,42] the nuclear Overhauser enhancement in rotating frame method (ROESY),[43,44] the indirectly detected heteronuclear single-bond $^1H-^{13}C$ correlation method (HSQC),[45−47] and the ^1H-detected heteronuclear multiple bond connectivity method (HMBC).[48,49] To obtain the diffusion ordered 2D spectroscopy (DOSY) spectra and to measure self-diffusion coefficients, we used a pulsed field gradients (stimulated echo) (PFG STE) sequence employing bipolar gradients and a longitudinal eddy current delay (LED).[50] The DOSY spectra were created using ILT protocol. NMR chemical shifts are given in ppm from the

(22) Rousset, A.; Chassagneux, F.; Paris, J. *J. Mater. Sci.* **1986**, *21*, 3111.
(23) Guillot, B.; Guendouzi, M. El; Rousset, A.; Tailhades, P. *J. Mater. Sci.* **1986**, *21*, 2926 .
(24) Ravindranathan, P.; Mahesh, G. V.; Patil, K. C. *J. Solid State Chem.* **1987**, *66*, 20.
(25) Tsumura, T.; Shimizu, A.; Inagaki, M. *J. Mater. Chem.* **1993**, *3*, 995.
(26) Peshev, P.; Tosxshev, A.; Gyurov, G. *Mater. Res. Bull.* **1989**, *24*, 33.
(27) Yamamoto, N.; Higashi, S.; Kawano, S.; Achiwa, N. *J. Mater. Sci. Lett.* **1983**, *2*, 525.
(28) Yamamoto, N.; Kawano, S.; Achiwa, N.; Higashi, S. *J. Jpn. Soc. Powder Powder Metall.* **1983**, *30*, 48.
(29) Pathak, A; Mukhopadhyay, D. K.; Prammanik, P. *Mater. Res. Bull.* **1992**, *27*, 155.
(30) Prabaharan, S. R. S.; Michael, M. S.; Kumar, T. P.; Mani, A.; Athinarayanswamy, K.; Gangadharan, R. *J. Mater. Chem.* **1995**, *5*, 1035.
(31) Rossen, E.; Reimers, J. N.; Dahn, J. R. *Solid State Ionics* **1993**, *62*, 53.
(32) Oh, I. H.; Hong, S. A.; Sun Y. K. *J. Mater. Sci.* **1997**, *32*, 3177.
(33) Barboux, P.; Tarascon, J. M.; Shokoohi, F. K. *J. Solid State Chem.* **1991**, *94*, 185.
(34) Garcia, B.; Barboux, P.; Ribot, F.; Kahn-Harari, A.; Mazerolles, L.; Baffler, N. *Solid State Ionics* **1995**, *80*, 111.
(35) Saadoune, I.; Delmas, C. *J. Mater Chem.* **1996**, *6*, 193.
(36) Zhecheva, E.; Stoyanova, R. *Solid State Ionics* **1993**, *66*, 143.
(37) Delmas, C.; Saadoune, I. *Solid State Ionics* **1992**, *53−56*, 370.
(38) Sun, Y. K.; Oh, I. H.; Hong, S. A. *J. Mater. Sci.* **1996**, *31*, 3617.
(39) Sun, Y. K.; Oh, I. H.; Hong, S. A. *J. Mater. Sci. Lett.* **1997**, *16*, 30.
(40) Walker, E. H., Jr.; Owens, J. W.; Etienne, M.; Walker, D. *Mater. Res. Bull.* **2002**, *37*, 1041.
(41) Rance, M.; Sorenson, O. W.; Bodenhausen, G.; Wagner, G.; Ernst, R. R.; Wuthrich, K. *Biochem. Biophys. Res. Commun.* **1983**, *117*, 479.
(42) Shaka, A. J.; Freeman, R. *J. Magn. Reson.* **1983**, *51*, 169.
(43) Bax, A.; Davis, D. G. *J. Magn. Reson.* **1985**, *61*, 306.
(44) Hwang, T. L.; Shaka, A. J. *J. Am. Chem. Soc.* **1992**, *114*, 3157.
(45) Norwood, T. J.; Boyd, J.; Heritage, J. E.; Soffe, N.; Campbell, I. D. *J. Magn. Reson.* **1990**, *87*, 488.
(46) Kay, L. E.; Keifer, P.; Saarinen, T. *J. Am. Chem. Soc.* **1992**, *114*, 10663.
(47) Palmer, A. G., III; Cavanagh, J.; Wright, P. E.; Rance, M. *J. Magn. Reson.* **1991**, *96*, 416.
(48) Summers, M. F.; Marzilli, L. G.; Bax, A. *J. Am. Chem. Soc.* **1986**, *108*, 4285.
(49) Bax, A.; Summers, M. F. *J. Am. Chem. Soc.* **1986**, *108*, 4285.
(50) Jerschow, A.; Muller, N. *Macromolecules* **1998**, *31*, 6573.

spectra obtained at 500 MHz in D20 at 25.0 ± 0.1 °C. Crystallographic data (excluding structure factors) for the structure in this paper have been deposited with the Cambridge Crystallographic Data Centre as supplementary publication CCDC 208196. Copies of the data can be obtained free of charge on application to CCDC, 12 Union Road, Cambridge, CB2 1EZ, UK.

Synthesis. *$Mn(C_3H_3O_2)_2{\cdot}(H_2O)_2$.* Manganese acetate (Aldrich Chemical Co.; 6.1273 g (25.00 mmol)) was dissolved in deionized water (100 mL). Next, 3.6030 g (50.00 mmol) of acrylic acid (Fischer Scientific) was added to the clear manganese acetate solution, and the mixture was refluxed for 30 min. The solution was then rotary evaporated (Buchler Instruments) to remove the solvent, and then dried over potassium hydroxide under vacuum overnight. A light pink solid resulted (4.9206 g, 99.89%). Elemental Anal. calcd for $Mn(C_3H_3O_2)_2{\cdot}(H_2O)_2$: 32.69% C, 4.02% H, and 23.57% Mn. Found: 32.35% C, and 3.98% H. The % manganese from pyrolysis was 23.81 wt %. IR (thin film, KBr plates, cm^{-1}): 3380 (s, br), 1639 (m), 1534 (s), 1432 (s), 1364 (m), 1275 (w), 1228 (w), 1061 (w), 988 (w), 962 (sh), 906 (w), 838 (m), and 779 (w).

$Sr(C_3H_3O_2)_2{\cdot}(H_2O)$. Acrylic acid (3.5735 g, 49.59 mmol) was added to a solution (6.5323 g, 24.58 mmol) of strontium hydroxide (Aldrich) that was dissolved in 100 mL of water, and the mixture was refluxed for 30 min. The solution was then rotary evaporated (Buchler Instruments) to remove the solvent, then dried under vacuum overnight. A white solid was obtained in a yield of 5.6444 g (99.96%). Elemental Anal. calcd: 29.82% C, 3.15% H, and 35.88% Sr. Found: 29.58% C, and 3.13% H. The % strontium from pyrolysis was 35.18 wt %. IR (thin film, KBr plates, cm^{-1}): 3336 (m, br), 1690 (m), 1639 (m, sh), 1540 (s), 1425 (s), 1363 (m), 1275 (m), 1061 (w), 1024 (w), 987 (w), 966 (sh), 902 (w), 832 (m), and 806(sh).

$La(C_3H_3O_2)_3{\cdot}(H_2O)_2$. Lanthanum acetate (Aldrich; 5.0849 g (16.09 mmol)) was dissolved in deionized water (100 mL) and refluxed for 30 min. Acrylic acid (3.5005 g, 48.57 mmol) was then added to the lanthanum acetate solution, and again the mixture was refluxed for 30 min. The solution was rotary evaporated to remove the solvent and then dried over potassium hydroxide under vacuum overnight. A white solid was obtained in a yield of 5.0926 g (98.70%). Elemental Anal. calcd: 28.22% C, 3.47% H, and 35.79% La. Found: 28.36% C, and 3.48% H. The % lanthanum from pyrolysis was 34.59 wt %. IR (thin film, KBr plates, cm^{-1}): 3369 (s, br), 1689 (sh), 1639 (m), 1525 (s), 1438 (s), 1368 (m), 1275 (w), 1061 (w), 1019 (sh), 988 (sh), and 835 (m).

Synthesis of $La_{0.8}Sr_{0.2}MnO_3$. Lanthanum acrylate (2.0249 g) was dissolved in 50 mL of deionized water and refluxed for 20 min. Then 2.90 mL of NH_4OH was added to the solution and refluxed for a few minutes. Next 5.30 mL of acrylic acid was added to this solution and the mixture was allowed to reflux overnight at low heat until the solution was homogeneous. Similarly, a manganese oxide precursor solution was obtained using 1.6190 g of manganese acrylate in 50 mL of deionized water, 9.10 mL of NH_4OH, and 16.81 mL of acrylic acid. The strontium oxide precursor solution was also prepared by following the same procedure using 0.5663 g of strontium acrylate, 50 mL of water, 2.72 mL of NH_4OH, and 5.00 mL of acrylic acid.

Each metal acrylate solution was then concentrated by rotary evaporation until a viscous gel was obtained. The lanthanum solution was then transferred with deionized water into a 500-mL round-bottom flask. Next, the strontium solution was washed into the lanthanum solution with deionized water. This two-compound solution was then rotary evaported until the solution was viscous again. The manganese acrylate solution was then added to the lanthanum/strontium solution with 100 mL of deionized water and the mixture was allowed to reflux overnight on low heat. The complete solution of lanthanum, strontium, and manganese was then rotary evaporated to remove all the solvent from the solution and to create a very viscous gel. The sample was then heated at 400 °C for 10 hours to convert it to $La_{0.8}Sr_{0.2}MnO_3$ (1.4661 g, 98.70%). IR (thin film, KBr plates, cm^{-1}): 3361 (m, br), 1639 (m), 1531 (s), 1432 (s), 1365 (m), 1275 (w), 1222 (w,sh), 1062 (w), 1020 (w), 988 (w), 960 (sh), 911 (w), and 834 (m).

Chart 1. 3,3′,3″-Nitrilotripropionic Acid

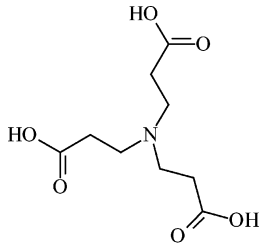

1

3,3′,3″-Nitrilotripropionic Acid. A round-bottom flask containing acrylic acid (743.2 g, 599.5 mmol) was stoppered and placed into the refrigerator overnight. A similar round-bottom flask containing ammonium hydroxide (24.2 g of 29.6% ammonia solution, which is 7.003 g of NH_3, 199.87 mmol) was also chilled overnight. The round-bottom flask containing the cold acrylic acid was then placed in an ice bath to maintain a temperature of approximately 0 °C. The ice bath was used because the reaction of acrylic acid and ammonium hydroxide is extremely exothermic. The cold ammonia hydroxide solution was slowly added (while stirring) to the cold acrylic acid. The solution was allowed to sit in the ice bath at approximately 0 °C for 30 min and then slowly brought to room temperature. Initial ^1H NMR of the material in solution indicated that the acrylic acid did not react with the ammonia hydroxide, so the solution was heated to boiling for 40 min. Peaks at 4.3 ppm (triplet), 3.3 ppm (triplet), 2.7 ppm (triplet), and 2.6 ppm (triplet) began to appear. Water was added to control gelling. After several hours of heating, the gel was rotary evaporated to remove excess water and dried over high vacuum to yield a white solid material (44.5 g, 95.52%). Colorless crystals were grown by slowly evaporating a solution containing the amino acid. ^1H (D_2O): δ(ppm) 6.037 J_{ab} (trans) = 17.4 Hz (doublet of doublets, 1 H, $O_2CC\mathbf{H_a}CH_2$), 5.966 J_{bc} (germinal) = 1.9 Hz (doublet of doublets, 1H, $CHC\mathbf{H_b}H_c$), and 5.594 J_{ac} (cis) = 10.1 Hz (doublet of doublets, 1H, $CHCH_b\mathbf{H_c}$). ^{13}C NMR: δ(ppm) 133.68 ($O_2C\mathbf{C}HCH_2$), 127.353($O_2CHC\mathbf{C}H_2$), and 175.40 ($O_2\mathbf{C}$-$CHCH_2$). Elemental Anal. calcd for $C_9H_{15}NO_6$: 40.43% C, 7.92% H, and 15.73% N. Found: 40.26% C, 8.04% H, and 15.20% N. IR (thin film, KBr plates, cm^{-1}): 3857 (w), 3809 (w), 3744 (w), 3420 (s, br), 3223 (sh), 2382 (w), 2124 (w), 1927 (w), 1842 (w), 1643 (m), 1547 (s), 1423 (m), 1360 (m), 1277 (w), 1227 (w), 1121 (w), 1060 (w), 988 (w), 891 (sh), 839 (sh), 661 (m, br), and 619 (sh).

Results and Discussion

Many studies dating back to the early 1950s have described the effects of ligand structure on the stability of aqueous metal complexes. Chaberek and Martell reported the acid dissociation constants of organic acids such as aspartic acid,[51,52] 3,3′,3″-nitrilotripropionic acid (NTP, Chart 1) **1**, nitrilotriacetic acid (NTA), and nitrilodipropionicacetic acid (NDAP), and the chelate stability constants of the corresponding carboxylates with cupric, nickelous, cobaltous, zinc, and cadmium ions.[53−55] Schwartzenbach et al. extensively studied the metal chelating tendencies of NTA and NDAP for alkaline earth ions.[56−58] Chelating amino acids are

(51) Miyamoto, S.; Schmidt, C. L. A. *J. Biol. Chem.* **1933**, *99*, 335.
(52) Batchelder, A. C.; Schmidt, C. L. A. *J. Phys. Chem.* **1940**, *44*, 893.
(53) Chaberek, S., Jr.; Martell, A. *J. Am. Chem. Soc.* **1952**, *74*, 5052.
(54) Chaberek, S., Jr.; Martell, A. *J. Am. Chem. Soc.* **1952**, *74*, 6021.
(55) Chaberek, S., Jr.; Martell, A. *J. Am. Chem. Soc.* **1952**, *74*, 2888.
(56) Schwartzenbach, G.; Kampitsch, E.; Steiner, R. *Helv. Chim. Acta* **1945**, *23*, 1133.

Scheme 1. Reaction Schematic of Ammonium Acrylate Undergoing the Anti-Markovnikov Addition

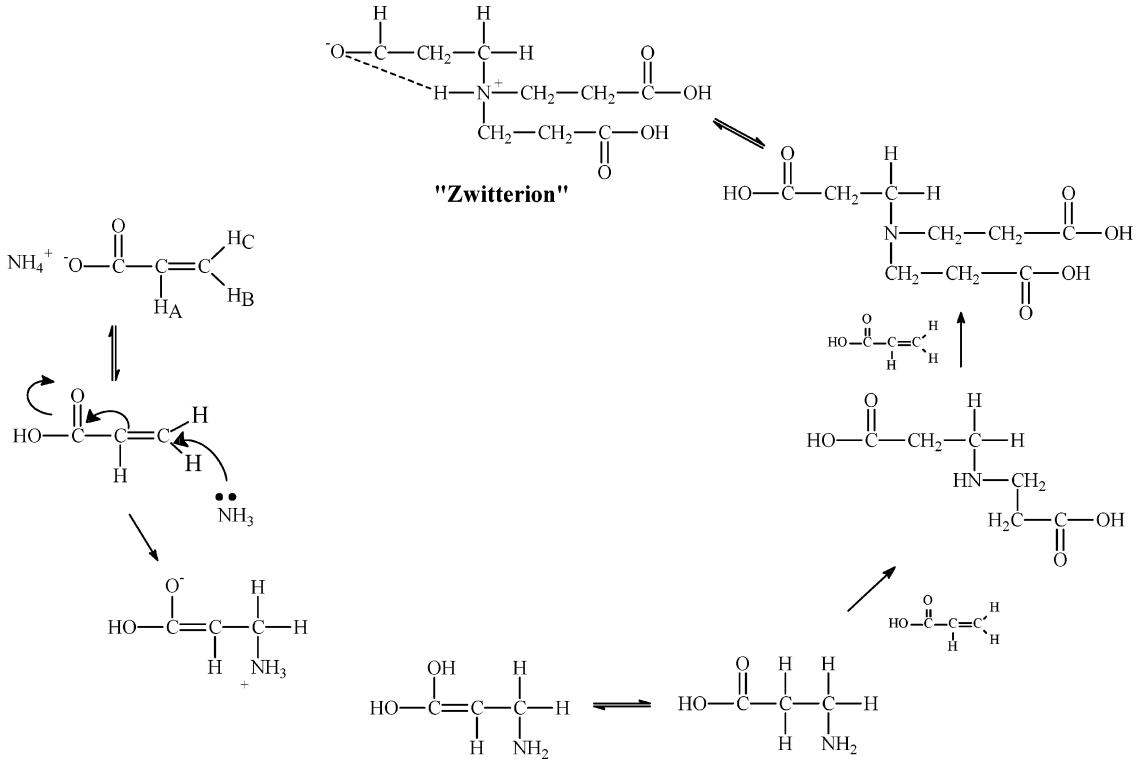

water-soluble and combine with the more basic metal ions, such as the alkaline earth metals. These same agents also exhibit an appreciable affinity for transition metals and other heavy metals ions.[56–58]

Recently, a low temperature precursor method has been developed by the Walker group[40] for the synthesis of nanocrystalline ternary oxide materials from an NTP precursor solution. Despite the fact that NTP has been studied and its crystal structure has been published, there have been no reports of methods of preparation of this compound. This report describes the synthesis of NTP **1** utilizing the novel ammonium acrylate salt. The reaction occurs in the NTP system due to the condensation of ammonia with the vinyl group of acrylic acid via an internal rearrangement, which is proposed to occur by the classic Michael addition mechanism shown in Scheme 1.

When the ammonium acrylate species is heated in the absence of water (or in the presence of the stoichiometric amounts of water produced in the neutralization reaction of acrylic acid with ammonium hydroxide), the NH_3 nucleophile attacks the double bond at the primary carbocation produced by electrons shifting toward the carbonyl through resonance to form an enolate ion. The amine formed, $HO_2CCH_2CH_2NH_2$, is more basic than the previous nucleophile, NH_3. This monosubstituted amine proceeds to attack another acrylic acid molecule to produce the di-substituted amine. The reaction continues until it terminates with the production of the trisubstituted amine, NTP. Due to the high degree of hydrogen bonding with water, NTP forms a viscous liquid that can absorb many times its own weight of water. Ammonium acrylate, NH_4A, salt was prepared by neutralization of ammonium hydroxide with acrylic acid in water. Proton NMR reveals that the ammonium and acrylate ions are completely solvated in water. With the application of heat, NH_4A undergoes a rearrangement to form a highly hydrogen bonded viscous amino acid. Since the amino acid readily forms hydrogen bonds with water, the amino acid has the ability to absorb many times its own weight in water. The water content was determined by dehydration experiments conducted in vacuo at 100 °C.

The presence of a weak IR absorption at 1643 cm^{-1} in the viscous amino acid compound confirms the presence of an intact carbon−carbon double bond, and consequently, the existence of unreacted or partially reacted amine species. Confirmation of structure is further corroborated by strong and broad O−H and N−H stretching frequencies appearing at 3419 cm^{-1}, and by the presence of strong symmetric and asymmetric bridging carboxylate frequencies appearing near 1547 and 1423 cm^{-1}, respectively. These frequencies are consistent with a deprotonated carboxylic acid.

Proton and carbon NMR spectroscopy is also consistent with the argument that the viscous amino acid exists as a mixture of completely and partially reacted species, as evidenced by the fact that chemical shifts of the vinylic hydrogen and carbon atoms are similar in both the starting material and the final product. A diffusion ordered 2D spectroscopy (DOSY) experiment preformed on the viscous amino acid distinguished four different species on the basis of their diffusion coefficients (Figure 1). The presence of an unsaturated species (diffusion coefficient = 8.2×10^{-10}), a saturated species (diffusion coefficient = 7.6×10^{-10}), a saturated species (diffusion coefficient = 4.9×10^{-10}), and a six-membered alanine H-ring species (diffusion coefficient

(57) Schwartzenbach, G.; Ackermann, H.; Ruckstuhl, P. *Helv. Chim. Acta* **1949**, *32*, 1175.
(58) Schwartzenbach, G.; Freitag, E. *Helv. Chim. Acta* **1951**, *34*, 1492.

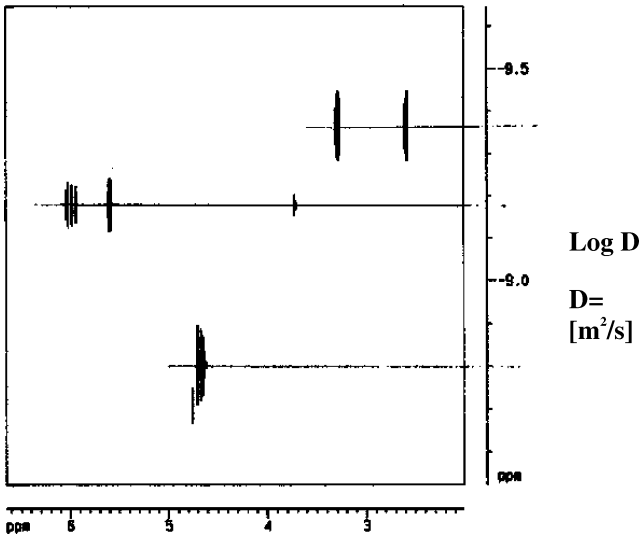

Figure 1. DOSY spectra of the ammonium acrylate gel.

$= 1.1 \times 10^{-11}$) was revealed. The ratio of the self-diffusion coefficients can be used to estimate the species size (assuming that the ratio of the diffusion coefficients is inversely proportional to the cube root of the relative volumes of the species). The results indicate that the four different species that compose the elaborate highly hydrogen bonded amine network move or diffuse through the solvent at different rates. Such conclusions are valid only if the different species have similar shapes. Therefore, a larger species should move or diffuse through the solvent at a slower rate than a species with a similar shape and a smaller size.

The proton NMR chemical shifts of the doublet of doublets at δ 6.037, 5.966, and 5.594 ppm (J_{ab} (trans) = 17.4 Hz, J_{bc} (germinal) = 1.9 Hz, and J_{ac} (cis) = 10.1 Hz) correspond to H_a, H_b, and H_c of the unsaturated species, suggesting the unsaturated species is the ammonium acrylate salt. The proton NMR chemical shifts of the triplets at δ 3.30 (J = 6.9 Hz) and 2.59 (J = 6.8 Hz) ppm correspond to the CH_2 groups of the propionic acid produced in the proposed Michael Addition reaction and thus confirm that the saturated species is 3,3′,3″-nitrilotripropionic acid. Single-bond $^1H-^{13}C$ correlation (HSQC) and ^1H-detected heteronuclear multiple bond connectivity (HMBC) experiments suggest that the saturated species are intermediate primary or secondary amine acids. The integration of the spectra indicates that the unsaturated species, saturated species, and the saturated species are in a 1:5:0.25 ratio, which suggests that the immediate primary or secondary amine is a short-lived species in the formation of 3,3′,3″-nitrilotripropionic acid.

Previous reports indicate that NTP forms an elaborate hydrogen-bonded amine network. The formation of intramolecular bonds results in the generation of two six-membered alanine H-rings,[59] (Figure 2), that are responsible for the broad peaks seen at δ 2.19, 1.72, and 1.56 ppm in the ^1H NMR. The magnitude of the diffusion coefficients obtained from the DOSY experiment is exactly what would be expected for a mixture of compounds with similar structures but varying molar

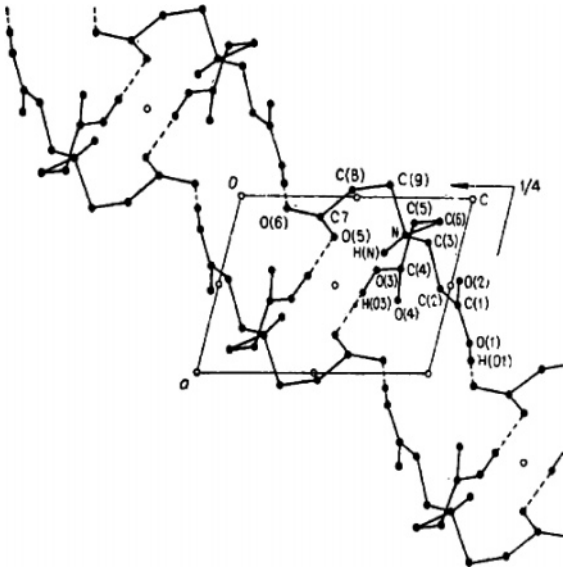

Figure 2. Projection of 3,3′,3″-nitrilotripropionic acid two-membered alanine H-rings along the [010] axis. Reprinted with permission from ref 59. Copyright 1984 Mezhdunar Kniga.

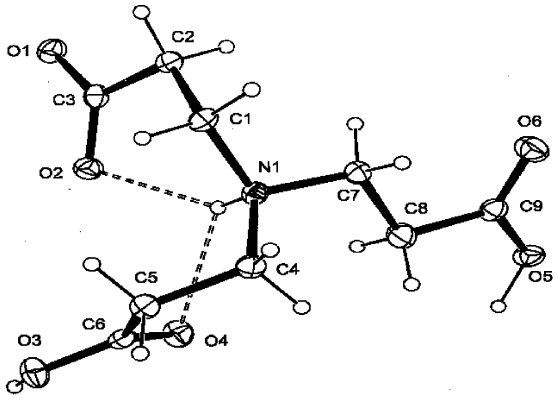

Figure 3. Crystal structure of the 3,3′,3″-nitrilotripropionic acid zwitterion.

mass (such as the four species found in the viscous amino acid).

An X-ray structure determination was made using a colorless crystal grown from a slowly evaporating aqueous solution containing the amino acid. The crystal of 3,3′,3″-nitrilotripropionic acid indicates the presence of a zwitterion with the N atom protonated and one of the COOH groups deprotonated. Intramolecular hydrogen bonding between the carboxylate and carboxylic acid of an adjacent molecule forms an extended H-bonded network shown in Figure 3. The proton on the amine forms an intramolecular hydrogen bond with the COOH group. The C−N bonds are lengthened by 0.03−0.04 Å as compared with the sum of the covalent radii (1.47 Å), which is typical of protonated nitrogen.[60] The nitrogen atoms are situated in a tetrahedral environment. The positions of both the carboxylate and carboxylic acid groups are in complete agreement with the results of a statistical treatment of the literature values for COO− and COOH groups.[61] The differences in the carbon−oxygen bond lengths of the carboxylate C−O groups found in similar complexes[59,62] are absent in

(59) Shkol'nikova, L. M.; Polyanchuk, G. V.; Dyatlova, N. M.; Polyakova, I. A. *Zh. Strukt. Khim.* **1984**, *26*, 153.

(60) Daly, J. J.; Wheatley, P. J. *J. Chem. Soc. A* **1967**, 212.
(61) Borthwick, P. W. *Acta Crystallogr. B* **1980**, *36*, 628.

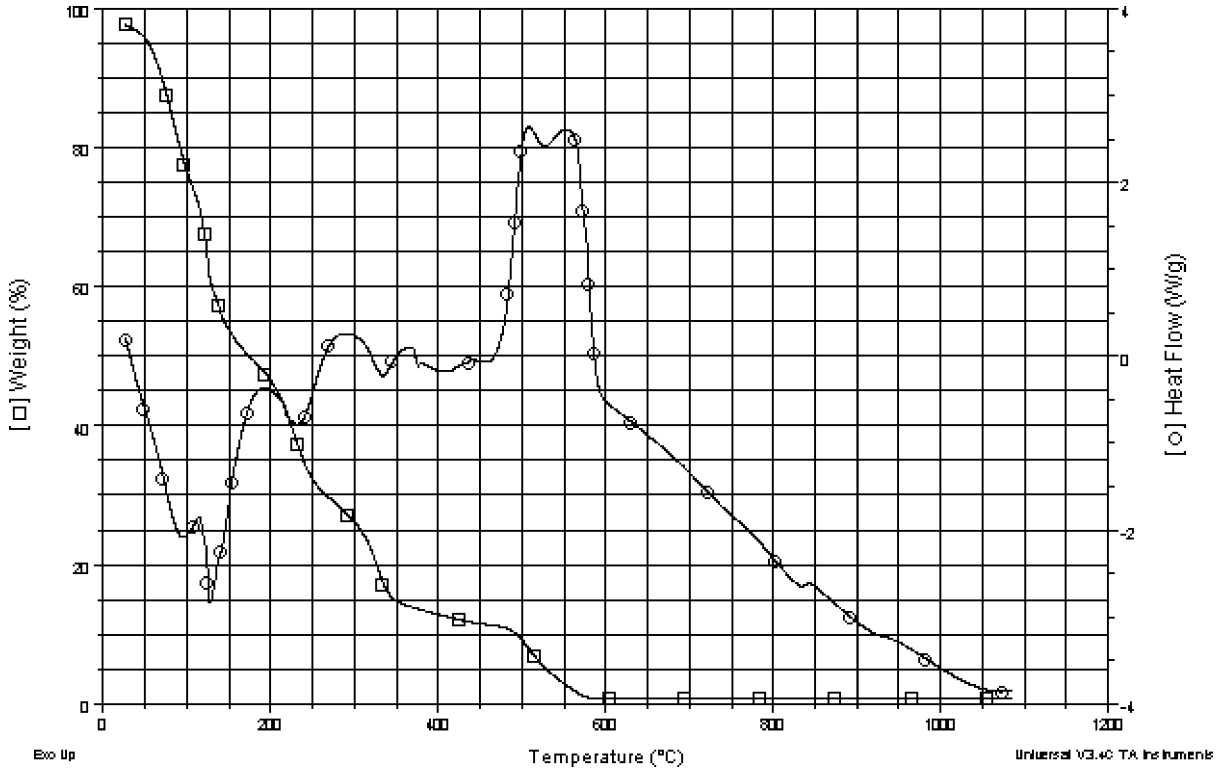

Figure 4. Thermogravimetric analysis (TGA/DSC) of the LSM precursor performed in air at a heating rate of 4 °C/min.

NTP, since both O atoms are acceptors and participate in the formation of hydrogen bonds also of the same length.

The C(8)−C(7), C(5)−C(4), and C(2)−C(1) bond lengths in the propionic groups of NTP are shorter than the corresponding C−C bond found in propionic acid (1.54 Å).[63] A similar shrinkage is observed in the sulfur analogue of NTP, methylenedithiopropionic acid.[64] The two intramolecular (N−H- -O) bonds, the geometry of which corresponds to the Hamilton criteria,[65,66] form a bifurcate bond. The N−H- - -O(2) bond, in which the O(2) atom functions as an acceptor, is shorter than the N−H- - -O(4) bond, O(4) being a carbonyl oxygen. The oxygen atom associated with the third propionic group is not a participant in intramolecular hydrogen bonding. A similar passive behavior was observed in one of the three acetate groups in nitrilotriacetic acid.[67]

When ordinarily insoluble metal acrylate salts are introduced to the viscous liquid amino acid solution, the nucleophilic amine reacts with the metal acrylate, which results in an elaborate network of amine connected metal propionates. The very homogeneous viscous precursor metal propionate liquid can easily be applied to a substrate.

The hydrated form of lanthanum acrylate, $La(C_3H_3O_2)_3 \cdot (H_2O)_2$, was prepared by performing a metathesis reaction of lanthanum acetate and acrylic acid in water. The degree of hydration was determined in vacuo by dehydration experiments at 100 °C. The infrared spectrum of this material indicated the presence of hydrogen-bonded water, as evidenced by the appearance of a strong and broad absorption at 3369 cm^{-1}. The IR spectrum also clearly indicated the presence of bidentate chelating (ν_{as} = 1525 cm^{-1} and ν_s = 1438 cm^{-1}) carboxylate groups, as well as a strong carbon=carbon double bond adsorption occurring at 1639 cm^{-1}.

The reaction of acrylic acid with strontium hydroxide in water yielded the strontium acrylate salt, $Sr(C_3H_3O_2)_2 \cdot (H_2O)$. The infrared spectrum of this material indicated the presence of hydrogen-bonded water, with a strong and broad absorption at 3336 cm^{-1}. The IR spectrum also confirmed the presence of bridging carboxylate groups (ν_{as} = 1540 cm^{-1} and ν_s = 1425 cm^{-1}), as well as a strong carbon=carbon double bond adsorption appearing near 1690 cm^{-1}. ^1H and ^{13}C NMR spectroscopic measurements indicated the presence of one type of acrylate ligand.

The salt of manganese acrylate, $Mn(C_3H_3O_2)_2 \cdot (H_2O)_2$, was prepared by the reaction of acrylic acid with manganese acetate in water. The degree of hydration was determined in vacuo by dehydration experiments at 100 °C. The infrared spectrum of this material indicated the presence of hydrogen-bonded water, as evidenced by the appearance of a strong and broad absorption at 3380 cm^{-1}. The IR spectrum also clearly indicated the presence of bidentate chelating (ν_{as} = 1534 cm^{-1} and ν_s = 1432 cm^{-1}) carboxylate groups, as well as a strong carbon=carbon double bond adsorption occurring at 1639 cm^{-1}.

Thermogravimetric analysis (TGA/DSC) (2960, TA Instruments) of the LSM precursor was performed in

(62) Gasparyan, A. V.; Obodovskaya, A. E.; Shkol'nikova, L. M.; Dyatlova, N. M. In *4th All Union Conference of Organic Crystallochemistry [in Russian]*; Zvenigorod, 1984; p 151.
(63) Strieter, F. J.; Templeton, D. H.; Scheuerman, F. R.; Sass, R. L. *Acta Crystallogr.* **1962**, *15*, 1233.
(64) Canonne, P.-J.; Boivin, J.-C.; Nowogrocki, G.; Thomas, D. *Acta Crystallogr. B* **1977**, *33*, 2550.
(65) Hamilton, W. C. *Structural Chemistry and Molecular Biology*; W. H. Freeman: San Francisco, CA, 1968.
(66) Koetzle, T. F.; Hamilton, W. C.; Tarthasavathy, R. *Acta Crystallogr. B* **1972**, *28*, 2083.
(67) Stanford, R. *Acta Crystallogr.* **1967**, *23*, 825.

air with a heating rate of 4 °C/min, Figure 4. The thermal decomposition of the LSM precursor in air occurs in several steps at 40−160 °C, 240−360 °C, and terminates at 360−600 °C. The TGA analysis of the LSM precursor indicated that the initial 18% mass loss in the temperature range of 40−160 °C corresponds to the removal of superficial and structural water in the novel gel precursor, which is accompanied by an endothermic peak at 125 °C in the DSC curve. The initial mass loss followed by a 43% mass loss that occurs in the temperature range 240−360 °C is associated with the combustion of the organic constituents in the LSM precursor, which is related to the exothermic peaks at 230 and 340 °C in the DSC curve. The exothermic peaks at 230 and 340 °C are a result of the decomposition of the acrylate constituents of LSM precursor, which decomposes similarly to polyacrylic acid (PAA). The final 2% mass loss that occurs from 360 to 600 °C indicates the combustion of the remaining organic constituents in the novel gel precursor. The mass at 600 °C in the TGA corresponded to the expected mass of the ceramic material (37%). The exothermic peak at 325 °C in the DSC curve is the crystallization phase change associated with the formation of LSM. While the chemical bonding of the cations to the polymeric network is destroyed during pyrolysis, the high viscosity of the LSM precursor results in low mobility, which prevents the different cations from segregating. Also, this elaborate network of amine connected metal propionates acted as fuel during pyrolysis. This is supported by the observation of the LSM precursor turning into fluffy grayish black foam shaped powder after heating to 300 °C. Therefore, it is assumed that during the pyrolysis there is little segregation of the various metal cations that are trapped in the char. Subsequently, the cations oxidize and begin to form crystallites of mixed metal cations oxides at 300 °C.

The XRD pattern of this material, obtained from bulk pyrolysis measurements at 400 °C, showed the material to be crystalline, which corresponded to a pervoskite type metal oxide. Heating beyond 400 °C resulted in a gradual crystallization of this perovskite. There was no evidence of the presence of any other strontium or manganese phases above this temperature. XRD analysis (Figure 5) demonstrated that nanocrystalline (8.0 nm) $La_{0.8}Sr_{0.2}MnO_3$ appeared when samples were heated at 400 °C for 10 hours. There were also traces of lanthanum oxycarbonate, $La_2O_2(CO_3)$, present presumably from the reaction of the highly reactive powder with atmospheric moisture and carbon dioxide. TGA analysis of the fired powder showed that it released absorbed water (1.11% by weight) between 25 and 500 °C and carbon dioxide (3.28 wt %) between 500 and 825 °C. The microstructure of the nanocrystalline $La_{0.8}Sr_{0.2}MnO_3$ sintered at 400 °C was investigated by transmission electron microscopy (TEM). A micrograph of the $La_{0.8}Sr_{0.2}MnO_3$ powder produced at 400 °C is shown in Figure 6. The grains throughout the sample can be classified as nanocrystalline with an average size of 25 nm and a narrow size distribution as depicted in the high-resolution TEM image. Thus, the XRD and TEM analysis suggest that the initially formed powder consists of slightly aggregated nanocrystalline grains of LSM. When the powder was further heated to 825 °C,

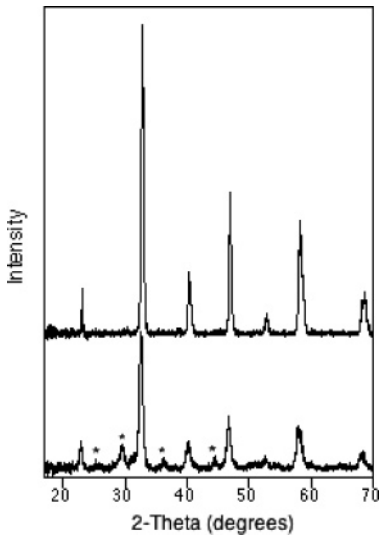

Figure 5. XRD of the LSM precursor heated to 400 °C (bottom) and 825° C (top). Starred reflections are due to $La_2O_2(CO_3)$ (ICDD 48-113). All others are due to $La_{0.8}Sr_{0.2}MnO_3$.

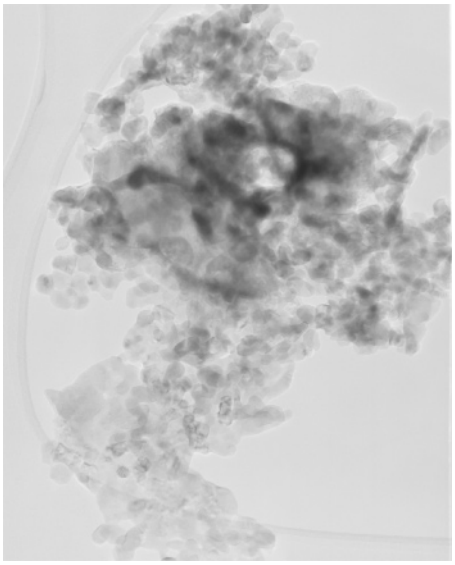

Figure 6. Micrograph of the $La_{0.8}Sr_{0.2}MnO_3$ powder produced at 400 °C.

XRD analysis (Figure 5) revealed that phase-pure $La_{0.8}Sr_{0.2}MnO_3$ was formed in the same size range (28.7 nm) as the secondary particles identified in the 400 °C sample by TEM. Thus, the precursor not only allows the low-temperature synthesis of $La_{0.8}Sr_{0.2}MnO_3$, but its mode of decomposition results in the controlled formation of a nanocrystalline oxide solid.

The $La_{0.8}Sr_{0.2}MnO_3$ precursor is unusual in that it generates an amorphous solid solution of lanthanum, manganese, and strontium oxides that yields a perovskite, the crystallinity of which is dependent on the sintering temperature and heating time. This property is ideal for certain applications. It is possible to generate oxide films with adjustable physical properties by spin-coating this perovskite precursor onto substrates and then sintering these substrates at temperatures chosen to achieve a desired outcome. It is very likely that the amorphous to crystalline phase change is susceptible to epitaxy, so that epitaxial $La_{0.8}Sr_{0.2}MnO_3$ films might be readily prepared.

Conclusion

The LSM NTP precursor is a solid that has the ability to absorb many times its own weight of water, to reversibly yield a hydrogel that has significant potential for the synthesis of ceramic nanocrystalline powders and thin films. When ordinarily insoluble metal acrylate salts are introduced to the viscous liquid amino acid solution, the nucleophilic amine reacts with the metal acrylate to generate a homogeneous polymeric network of amine-connected metal propionates via a Michael addition reaction. The resulting viscous precursor can be easily applied to a substrate and fired to yield ceramic thin films. The precursor is not only amenable to processing by MOD into different morphologies, but it also converts to an amorphous oxide at 400 °C and then slowly crystallizes to LSM at the same temperature. Heating this material to a variety of temperatures allows the careful tailoring of the crystalline size of the product LSM. However, the upper size limit is restricted to ca. 25 nm by the size of the agglomerates formed in the initial deposition process. The synthesis of LSM using the method discussed in this report provides a preferred alternative synthetic route that is innovative, affordable, and versatile for the preparation of ceramic oxides with particle diameter ranges from 8 to 25 nm.

Acknowledgment. This research was made possible by grants supplied by the State of Louisiana's EPSCoR (NSF/LEQSF (2001-04) RII-03), and the National Science Foundation's HBCU-UP program (Cooperative Agreement HRD-9815451) at Southern University. We wish to thank the Materials Characterization Center (MC^2) of Louisiana State University for the TEM measurements. This center is supported by grants from the National Science Foundation, DMR-9871417, and the Louisiana Board of Regents. We thank Dr. Allen W. Apblett for XRD measurements at OSU and for the helpful discussions. We thank Dr. K. Maskos for the NMR measurements that were performed at the Coordinated Instrumentation Facility, Tulane University, New Orleans, LA. We thank Dr. Frank Fronzcek of the chemistry department, Louisiana State University, Baton Rouge, LA for the single-crystal X-ray analyses. The purchase of the diffractometer was made possible by grant LEQSF(1999-2000)-ESH-TR-13, administered by the Louisiana Board of Regents.

Supporting Information Available: Crystallographic data (cif). This material is available free of charge via the Internet at http://pubs.acs.org..

CM0489385